ISSN 0915-633X

NATIONAL INSTITUTE FOR FUSION SCIENCE

Molecular Dynamics of Structure Organization of Polyampholytes

M. Tanaka, A. Yu Grosberg and T. Tanaka

(Received - Aug. 26, 1998)

NIFS-558 Sep. 1998

RESEARCH REPORT
NIFS Series

NAGOYA, JAPAN

Molecular Dynamics of Structure Organization of Polyampholytes

Motohiko Tanaka[1], A.Yu Grosberg[2,3], and Toyoichi Tanaka[2]

[1] National Institute for Fusion Science, Toki 509-5292, Japan
[2] Massachusetts Institute of Technology, Cambridge, MA 02139, USA
[3] Institute of Biochemical Physics, Russian Acad. Sci., Moscow 117977, Russia

Abstract

The dynamics and equilibrium of charged polymers of random co-polymerization (polyampholytes) are studied for both the single-chain and multichain cases with the use of molecular dynamics simulations. Nearly neutral single-chain polyampholyte has three temperature regimes, which are characterized by an elongated Gaussian coil, a transition between the coil and globular states, and a very dense globule for high, medium and low temperatures, respectively. The gyration radius of polyampholytes shows a hysteresis against slow cyclic temperature changes under the Coulomb and attractive short-range forces. The multichain polyampholyte forms a globule at low temperature and is composed of wall-bound separated chains at high temperature. The polyampholyte chains are overlapped above certain concentration or below a critical temperature due to the Coulomb force. Added salt ions screen the electric field between the monomers and make the polyampholyte soluble when density of the salt is comparable to that of the polyampholyte.

Keywords: Strongly-coupled Coulomb system, electrically charged polymers, multichain, polyelectrolyte, polyampholyte, hysteresis, folding process, salt electrolyte solution.

I. Introduction

The polymers that are composed of electrically charged monomers have a wide range of industrial applications. They are also important building blocks of live organisms such as nucleic acids and DNA. Because of the microscopic scales of Angstrom ranges, these polymers constitute *a strongly-coupled system*, where the Coulomb energy prevails over the thermal energy, $e^2/\epsilon aT \geq 1$. The charged polymers are classified into two typical groups (or regimes) called *polyelectrolyte* and *polyampholyte*. The former that consists of monomers of one charge sign takes an elongated conformation at equilibrium due to electrostatic repulsive force, which is usually surrounded by a cloud of neutralizing counter-ions. The structure of the latter, that includes nearly equal number of positively and negatively charged monomers, is quite variable upon charge sequences, temperature and existence of salt.

Recent studies of polyampholytes are mostly concerned the quenched ones whose charge state and sequence are predetermined by the synthesis chemistry[1]. The properties of these polymers were extensively studied experimentally[1,2], theoretically[3–5], and also numerically[6–9]. Here, we present simulation results of a dynamical process, formation and

relaxation to equilibrium conformations, and the effect of added salt by means of molecular dynamics (MD) simulations[7,8]. The motion of charged polymers in a thermal solution (such as water) is described by

$$m d\mathbf{v}_i/dt = \mathbf{F}_{LR}(\mathbf{r}_i) - (3T/a^2)(2\mathbf{r}_i - \mathbf{r}_{i+1} - \mathbf{r}_{i-1}) + \mathbf{F}_{th} - \nu m \mathbf{v}_i, \quad (1)$$

$$d\mathbf{r}_i/dt = \mathbf{v}_i. \quad (2)$$

These are a set of Langevin equations for N monomers. Here, $\mathbf{r}_i$ and $\mathbf{v}_i$ are the position and velocity of the i-th monomer ($i = 1 \sim N$) at a time t, respectively, T the temperature, a the normalization length close to the bond length. The long-range Coulomb force $\mathbf{F}_{LR}$ is calculated by direct sums among the monomers,

$$\mathbf{F}_{LR}(\mathbf{r}_i) = \sum_j Z_i Z_j e^2 \hat{\mathbf{r}}_{ij}/\epsilon |\mathbf{r}_i - \mathbf{r}_j|^2, \quad (3)$$

where $Z_i e$ is charge state, ϵ is electrical permitivity, and $\hat{\mathbf{r}}_{ij}$ is a unit vector along $\mathbf{r}_i - \mathbf{r}_j$. The last two terms in Eq.(1), which are random thermal kicks and momentum absorption executed by surrounding medium, equilibrate polyampholytes in solution. The most important controlling parameter is the electrostatic coupling constant Γ (or temperature T),

$$\Gamma = e^2/\epsilon a T. \quad (4)$$

Other implicit parameters are the exclusion radius of monomers a_{col}, the number of chains and monomers, and charge sequence of the chains.

II. Single-Chain Polyampholytes

The effect of unbalanced charge on the structure of polyampholytes[7] is depicted in Fig.1. Equilibrium conformations in the bird's-eye view plots and time histories of the gyration radius,

$$R_g = \left(\frac{1}{N} \sum_{j=1}^{N} (\mathbf{r}_j - < \mathbf{r} >)^2 \right)^{1/2}, \quad (5)$$

are shown on the left and right columns, respectively. The excess charge $\delta N = N_+ - N_-$ in a polyampholyte is (a) below, (b) just, and (c) above the critical value $\delta N_0 = N^{1/2}$; the temperature is medium $T/T_0 \sim 1$ (see Fig.2). When the charge imbalance is smaller than δN_0, the polyampholyte chain forms a globule. The relaxation time is roughly $200\omega_p^{-1}$, with $\omega_p \cong (2\pi e^2/ma^2)^{1/2}$ the plasma frequency. The above relaxation time falls in *a microsecond* range for the CH_2 monomer in pure water ($\epsilon = 80$). Beyond the critical charge imbalance, the chain takes a stretched conformation that resembles polyelectrolytes.

The temperature dependence is seen in the gyration radius for balanced polyampholytes. The gyration radius increases with temperature in Fig.2, where we find the low ($T < T_0$), medium, and high ($T > T_0$) temperature regimes, where the base temperature is defined by $e^2/\epsilon a T_0 = 1$. These regimes are characterized by a dense and loose globules, and an elongated Gaussian coil, respectively. The elongated coil at high temperature is not stationary, but repeats contraction and stretching motions.

These high and medium temperature regimes correspond to *the high and low temperature regimes* of the Flory theory[4] of the Θ solvent. The dense globule at low temperature, which results from compact folding of the chain arms – in good analogy with *protein folding*[10], was first obtained by the present MD simulation of non-lattice type[7]. The velocity distribution of the monomers is almost Gaussian $\exp(-v^2)$, which shows thermal equilibration of the globule.

The volume of a polyampholyte undergoes a hysteresis against slow cyclic temperature changes when the long-range Coulomb and attractive short-range forces cooperate[7]. If we start from a compact globule at low temperature in Fig.3, the polyampholyte keeps a small volume until the critical temperature is reached at $T = T_1$, where the vol-

ume jumps up due to unfolding of the chain. In the reverse phase back from high temperature ($T > T_0$), the volume takes a larger value than for the first (rising) phase until the polyampholyte suddenly collapses into a globule at $T = T_2$, with $T_1 > T_2$. This phenomenon reveals existence of two local energy minima around the critical temperature. Despite the hysteresis, the whole process is reversible unless a dissipation term other than viscosity in Eq.(1) is introduced. Precise descriptions are found in Ref.7.

III. Multi-Chain Polyampholytes

The time histories of the gyration radius of the whole system (chains) $R_{g,sys}$, the average of gyration radii of the chains R_{g1}, and the x-component velocity of one specific monomer are shown in Fig.4 for the multichain polyampholyte at high temperature[8]. Here, the polyampholyte is composed of eight 32-mer chains, each of which has a random charge sequence. The gyration radius of each chain does not change appreciably. But, the system gyration radius increases to a wall-bound equilibrium in $\tau_{eq} \sim 200\omega_p^{-1}$. A large increase in the size of polyampholyte is attributed to separation of the chains, which is a new feature of *multichain polyampholytes* compared to the single-chain ones.

The equilibrium conformations of multichain polyampholytes are shown for (a) high ($T/T_0 \sim 1$), and (b) low ($T/T_0 = \frac{1}{8}$) temperatures in Fig.5. The conformation at high temperature consists of wall-bound separated chains with a large void space among the chains, whereas that at low temperature is a collapsed globule resembling that of a single-chain polyampholyte. At high temperature, the gyration radius R_{g1} of each chain and the velocity of monomers undergo slow oscillations compared to the friction time ν^{-1}. The oscillations of R_{g1} which corresponds to folding /unfolding motion of the chain occurs simultaneously with gather and scatter motion of the chains. On the other hand, at low temperature in (b), the gyration radius R_{g1} does not show oscillations, which implies the liquid-like nature of a collapsed globule.

A brief summary is given here on the effect of specific charge sequences[8]. Thermodynamically, it was shown that a charged polymer with an alternating sequence is very different from one with a random sequence[5]. The present MD simulation finds that this is true for multichain polyampholytes with a completely alternating sequence. However, polyampholytes with a longer alternating interval whose block length (of the equal-sign charged monomers) is as small as four already behave like polyampholytes with random sequences[8]. Therefore, only the charge sequence of the block length one or two should be regarded as special.

The gyration radius and the filling index $\zeta = N_c^{1/3} R_{g1}/R_{g,sys}$ (N_c: the number of chains) of multichain polyampholytes depend on stiffness, molecular weight and the number of the chains. The critical temperature at which chain overlapping occurs is proportional to the molecular weight of the chains, $T_* \sim M_w$. Detailed results are described in Ref.8.

IV. The Effect of Salt

Addition of salt to a polyampholyte solution is known to enhance its dissolution in pure water[1]. A new set of molecular dynamics simulations are performed for the system consisting of multichain polyampholyte and free salt ions[8]. The salt ions are represented by the same number of positive and negative free counter-ions whose mass and charge are identical with those of the polyampholyte monomers. A typical equilibrium conformation of the polyampholyte is depicted in Fig.6, where scattered small pluses and dots are salt ions. The surface of the globule is

now quite fuzzy due to the presence of large number of the salt ions. This is clearly contrasted to the dense globule shown in Fig.5(b) under the same temperature and without salt.

The denseness of the polymer chains (or, the degree of chain overlapping) is well quantified by the *filling index* $\zeta = N_c^{1/3} R_{g1} / R_{g,sys}$, where N_c is a number of chains composing of the polyampholyte, R_{g1}, $R_{g,sys}$ the gyration radii of each chain and all the chains, respectively. This value equals or exceeds unity, $\zeta \geq 1$, when the chains closely overlap each other; it becomes small for the polymers of separated chains. Thus, we can judge that *the polymer is soluble* if the filling index becomes less than unity, $\zeta < 1$.

Figure 7 shows the filling index ζ for the multichain polyampholytes in salt-free solvent (triangles), and in salt aqueous solution (filled and open circles). Quite evidently, the value of the filling index is reduced in solutions with salt ions. The charge density with 512 salt ions is comparable to that of the polyampholyte inside the globule (or chain clouds). Half the density of the salt ions is still effective at high temperature, as the polyampholyte takes a larger volume having less charge density; it is less effective at low temperature. As has been shown clearly in Fig.7, the added salt ions act to screen the attractive electric field and separate the chains, which causes dissolution and swelling of polyampholytes[5,8].

The effect of salt can be approximately treated by means of enhanced electrical permitivity ϵ in Eqs.(1)-(3). However, at low temperature when a dense globule has been formed, the subtlety of added salt including the relaxation time is properly described only with the use of molecular dynamics simulations[8]. For example, unfolding of the globule due to addition of salt occurs by one order of magnitude more slowly than for the case with enhanced electrical permitivity. This is because the size of the salt ions is non-negligible compared to that of the void space among chained monomers of polyampholytes.

Acknowledgements

One of the authors (M.T.) would like to thank Dr.S.J.Candau, Dr.J.F.Joanny, and Dr.T.Hatori for constructive discussions.

References

1. References in F.Candau and J.F.Joanny, *Encyclopedia of Polymeric Materials, 7*, 5476 (edited by J.C.Salomone, CRC Press, Boca Raton, 1996).
2. J.M.Corpart and F.Candau, *Macromolecules, 26*, 1333 (1993).
3. P.G.Higgs and J.-F.Joanny, *J.Chem. Phys., 94*, 1543 (1990).
4. A.V.Dobrynin and M.Rubinstein, *J.de Phys.II, 5*, 677 (1995).
5. R.Everaers, A.Johner, and J.-F.Joanny, *Macromolecules, 30*, 8478 (1997).
6. Y.Kantor, M.Kardar and H.Li, *Phys. Review, E49*, 1383 (1994).
7. M.Tanaka, A.Yu Grosberg, V.S.Pande, and T.Tanaka, *Phys.Review, E56*, 5798 (1997).
8. M.Tanaka, A.Yu Grosberg, and T.Tanaka, *50th Yamada Conference - Polyelectrolytes '98* (Inuyama, May 31 - June 4, 1998).
9. H.Shiessel and A.Blumen, *Phys.Review E57, in press.*
10. *Protein Folding*, edited L.M. Gierasch and J. King (Amer. Assoc. for Advance. Sci., Washington D.C., 1989).

Figure Captions

Figure 1. Effect of unbalanced charge is shown by equilibrium conformations and

time histories of gyration radius, for (a) nearly neutral, (b) mirginal, and (c) non-neutral polyampholytes of 256-mers at the temperature $T = \frac{1}{2}T_0$. The conformation for (c) is reduced to 53% that of the real size.

Figure 2. Temperature dependence of gyration radius for the neutral 64, 128, and 256-mer polyampholytes. Three different regimes are identified at low, medium, and high temperatures.

Figure 3. A hysteresis of the gyration radius against slow cyclic temperature changes for a single-chain 64-mer polyampholyte under the Coulomb and attractive short-range forces.

Figure 4. Time histories of the system gyration radius $R_{g,sys}$, the gyration radius of each chain $R_{g,1}$, and one component of monomer velocity V_{x1} for the multichain polyampholyte (eight 32-mers) at the temperature $T/T_0 \sim 1$.

Figure 5. Equilibrium conformations of multichain polyampholytes for (a) high, and (b) low temperatures are wall-bound separated chains and a dense globule, respectively.

Figure 6. The effect of salt ions is seen in a loosened globule of multichain polyampholyte at low tempwerature $T = \frac{1}{8}T_0$. Small dots and pluses stand for negative and positive salt ions, respectively.

Figure 7. The filling index, $\zeta = N_c^{1/3} R_{g1}/R_{g,sys}$, is depicted for three cases with 512, 256, and no salt ions. The condition $\zeta \geq 1$ corresponds to overlapping of the polyampholyte chains.

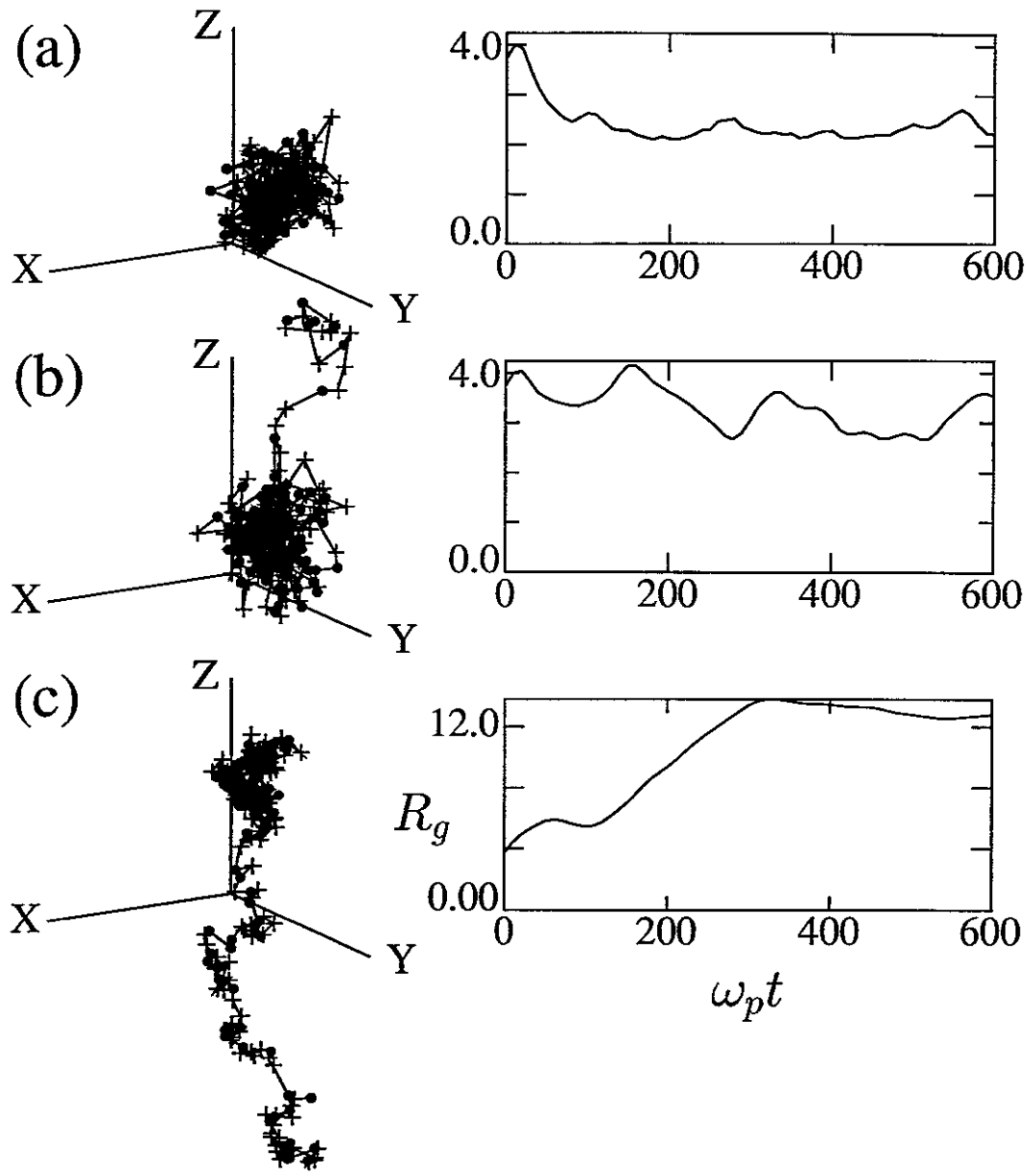
(a)
Z
X
Y
4.0
0.0
0
200
400
600
(b)
Z
X
Y
4.0
0.0
0
200
400
600
(c)
Z
X
Y
12.0
R_g
0.00
0
200
400
600
$\omega_p t$

Fig. 1

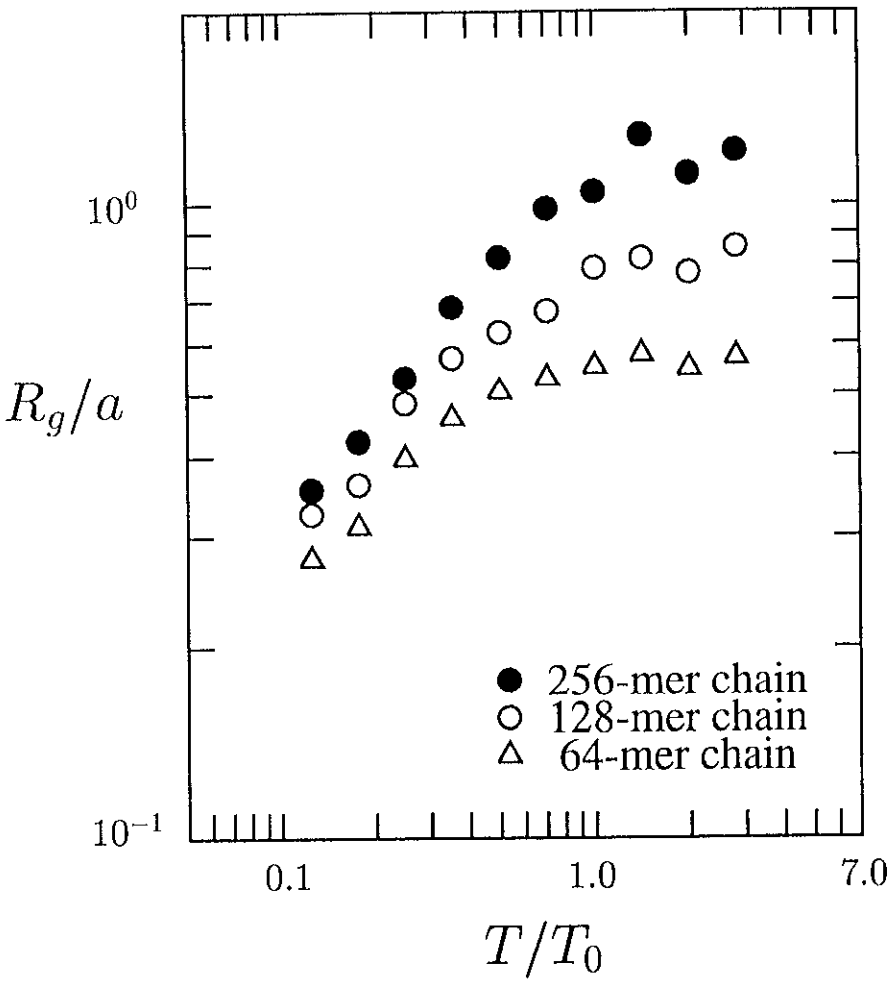
10^0
10^{-1}
R_g/a
0.1
1.0
7.0
T/T_0
256-mer chain
128-mer chain
64-mer chain

Fig. 2

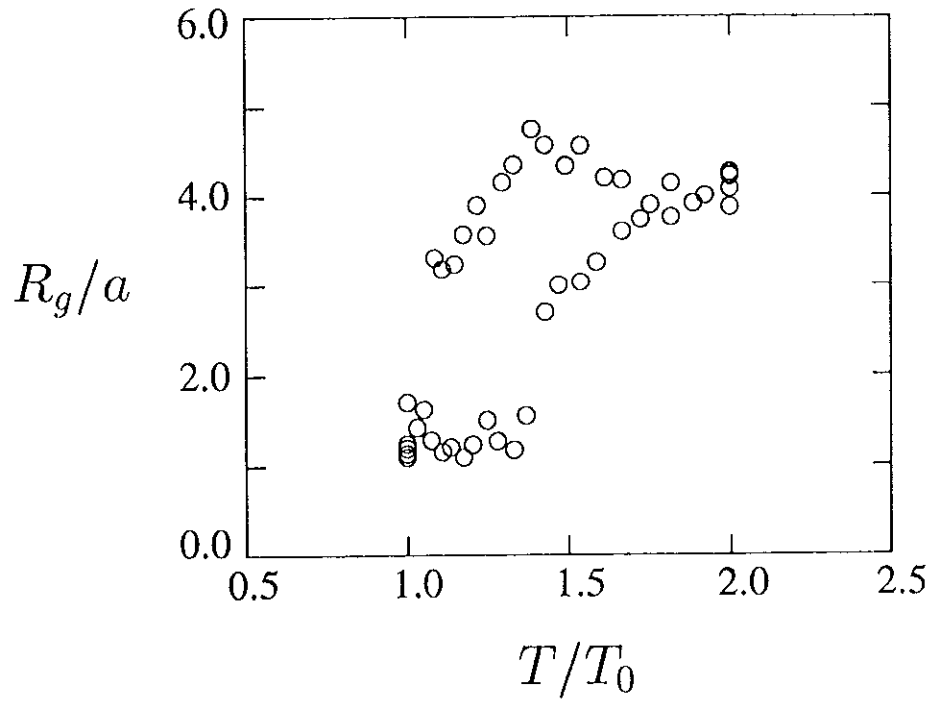
6.0
4.0
2.0
0.0
R_g/a
0.5
1.0
1.5
2.0
2.5
T/T_0

Fig. 3

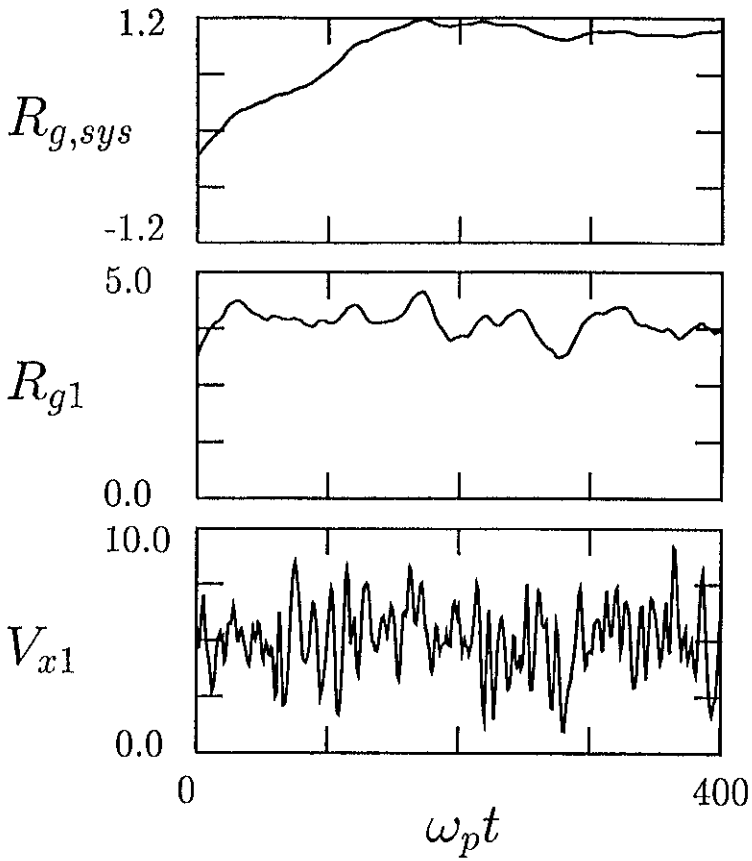

Fig. 4

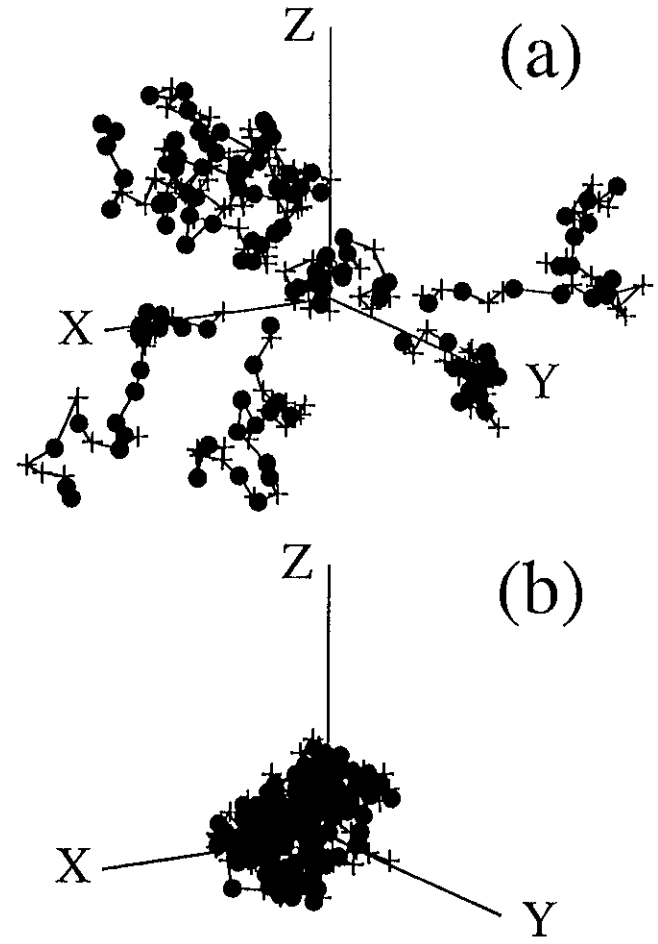

Fig. 5

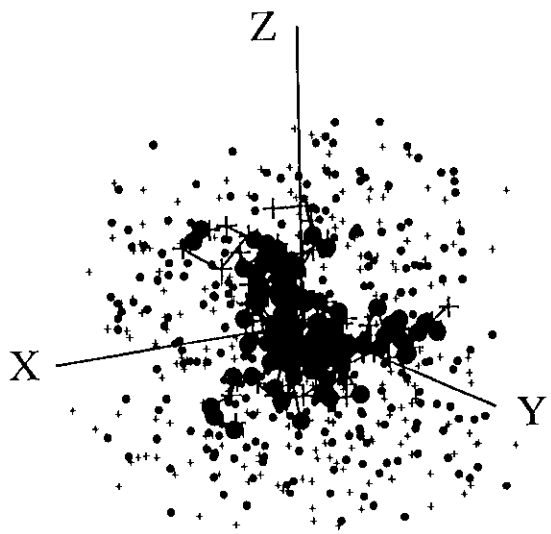
Z
X
Y

Fig. 6

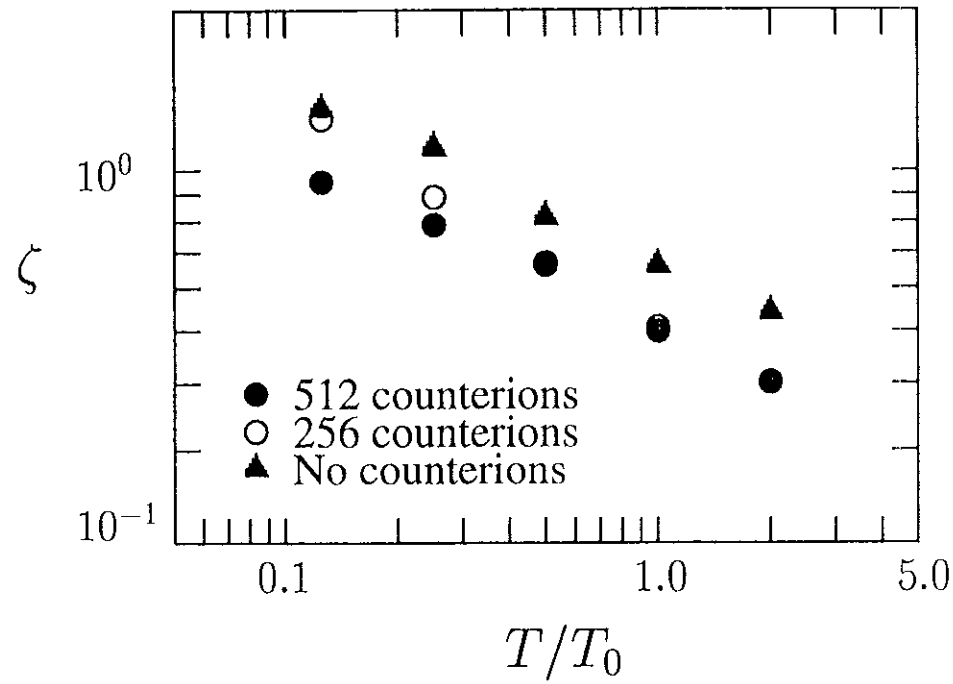
10^0
10^{-1}
ζ
0.1
1.0
5.0
T/T_0
512 counterions
256 counterions
No counterions

Fig. 7

Recent Issues of NIFS Series

NIFS-522 M Yokoyama, N Nakajima and M Okamoto,
Realization and Classification of Symmetric Stellarator Configurations through Plasma Boundary Modulations, Dec 1997

NIFS-523 H. Kitauchi,
Topological Structure of Magnetic Flux Lines Generated by Thermal Convection in a Rotating Spherical Shell; Dec. 1997

NIFS-524 T. Ohkawa,
Tunneling Electron Trap; Dec 1997

NIFS-525 K. Itoh, S -I. Itoh, M. Yagi, A. Fukuyama,
Solitary Radial Electric Field Structure in Tokamak Plasmas; Dec. 1997

NIFS-526 Andrey N. Lyakhov,
Alfven Instabilities in FRC Plasma; Dec 1997

NIFS-527 J. Uramoto,
Net Current Increment of negative Muonlike Particle Produced by the Electron and Positive Ion Bunch-method; Dec. 1997

NIFS-528 Andrey N. Lyakhov,
Comments on Electrostastic Drift Instabilities in Field Reversed Configuraiton; Dec. 1997

NIFS-529 J. Uramoto,
Pair Creation of Negative and Positive Pionlike (Muonlike) Particle by Interaction between an Electron Bunch and a Positive Ion Bunch; Dec 1997

NIFS-530 J. Uramoto,
Measuring Method of Decay Time of Negative Muonlike Particle by Beam Collector Applied RF Bias Voltage; Dec. 1997

NIFS-531 J. Uramoto,
Confirmation Method for Metal Plate Penetration of Low Energy Negative Pionlike or Muonlike Particle Beam under Positive Ions, Dec. 1997

NIFS-532 J. Uramoto,
Pair Creations of Negative and Positive Pionlike (Muonlike) Particle or K Mesonlike (Muonlike) Particle in H2 or D2 Gas Discharge in Magnetic Field, Dec. 1997

NIFS-533 S Kawata, C. Boonmee, T. Teramoto, L. Drska, J. Limpouch, R. Liska, M Sinor,
Computer-Assisted Particle-in-Cell Code Development; Dec. 1997

NIFS-534 Y. Matsukawa, T. Suda, S. Ohnuki and C. Namba,
Microstructure and Mechanical Property of Neutron Irradiated TiNi Shape Memory Alloy, Jan. 1998

NIFS-535 A. Fujisawa, H. Iguchi, H. Idei, S. Kubo, K. Matsuoka, S. Okamura, K Tanaka, T Minami, S Ohdachi, S. Morita, H Zushi, S Lee, M. Osakabe, R. Akiyama, Y. Yoshimura, K Toi, H. Sanuki, K. Itoh, A. Shimizu, S Takagi, A Ejiri, C. Takahashi, M. Kojima, S Hidekuma, K. Ida, S. Nishimura, N. Inoue, R. Sakamoto, S.-I. Itoh, Y. Hamada, M Fujiwara,
Discovery of Electric Pulsation in a Toroidal Helical Plasma; Jan 1998

NIFS-536 Lj.R. Hadzievski, M.M Skoric, M. Kono and T. Sato,
Simulation of Weak and Strong Langmuir Collapse Regimes, Jan. 1998

NIFS-537 H Sugama, W. Horton,
Nonlinear Electromagnetic Gyrokinetic Equation for Plasmas with Large Mean Flows; Feb. 1998

NIFS-538 H. Iguchi, T.P. Crowley, A. Fujisawa, S Lee, K. Tanaka, T. Minami, S. Nishimura, K. Ida, R. Akiyama, Y. Hamada, H , Idei. M. Isobe, M. Kojima, S. Kubo, S. Morita, S. Ohdachi, S. Okamura, M Osakabe, K Matsuoka, C Takahashi and K. Toi,
Space Potential Fluctuations during MHD Activities in the Compact Helical System (CHS); Feb. 1998

NIFS-539 Takashi Yabe and Yan Zhang,
Effect of Ambient Gas on Three-Dimensional Breakup in Coronet Formation Process;

Feb. 1998

NIFS-540 H. Nakamura, K. Ikeda and S. Yamaguchi,
Transport Coefficients of InSb in a Strong Magnetic Field; Feb. 1998

NIFS-541 J. Uramoto,
Development of ν_μ Beam Detector and Large Area ν_μ Beam Source by H_2 Gas Discharge (I); Mar. 1998

NIFS-542 J. Uramoto,
Development of bar{ν}$_\mu$ Beam Detector and Large Area bar{ν}$_\mu$ Beam Source by H_2 Gas Discharge (II); Mar. 1998

NIFS-543 J. Uramoto,
Some Problems inside a Mass Analyzer for Pions Extracted from a H_2 Gas Discharge, Mar. 1998

NIFS-544 J. Uramoto,
Simplified ν_μ bar{ν}$_\mu$ Beam Detector and ν_μ bar{ν}$_\mu$ Beam Source by Interaction between an Electron Bunch and a Positive Ion Bunch; Mar. 1998

NIFS-545 J. Uramoto,
Various Neutrino Beams Generated by D_2 Gas Discharge; Mar.1998

NIFS-546 R. Kanno, N. Nakajima, T. Hayashi and M. Okamoto,
Computational Study of Three Dimensional Equilibria with the Bootstrap Current; Mar. 1998

NIFS-547 R. Kanno, N. Nakajima and M. Okamoto,
Electron Heat Transport in a Self-Similar Structure of Magnetic Islands; Apr. 1998

NIFS-548 J.E. Rice,
Simulated Impurity Transport in LHD from MIST; May 1998

NIFS-549 M.M. Skoric, T. Sato, A M. Maluckov and M.S. Jovanovic,
On Kinetic Complexity in a Three-Wave Interaction; June 1998

NIFS-550 S. Goto and S. Kida,
Passive Saclar Spectrum in Isotropic Turbulence: Prediction by the Lagrangian Direct-interaction Approximation; June 1998

NIFS-551 T. Kuroda, H. Sugama, R. Kanno, M. Okamoto and W. Horton,
Initial Value Problem of the Toroidal Ion Temperature Gradient Mode ; June 1998

NIFS-552 T. Mutoh, R. Kumazawa, T. Seki, F. Simpo, G. Nomura, T. Ido and T. Watari,
Steady State Tests of High Voltage Ceramic Feedthoughs and Co-Axial Transmission Line of ICRF Heating System for the Large Helical Device ; June 1998

NIFS-553 N. Noda, K. Tsuzuki, A. Sagara, N. Inoue, T. Muroga,
oronaization in Future Devices -Protecting Layer against Tritium and Energetic Neutrals-: July 1998

NIFS-554 S. Murakami and H. Saleem,
Electromagnetic Effects on Rippling Instability and Tokamak Edge Fluctuations; July 1998

NIFS-555 H. Nakamura, K. Ikeda and S. Yamaguchi,
Physical Model of Nernst Element; Aug. 1998

NIFS-556 H. Okumura, S. Yamaguchi, H. Nakamura, K. Ikeda and K. Sawada,
Numerical Computation of Thermoelectric and Thermomagnetic Effects; Aug. 1998

NIFS-557 T. Yasuhiko, O. Masaki, T. Katsuyoshi, O. Yoshihide, K. Osamu, A. Eiji, K. Toshikazu, A. Ryuichi and T. Masanobu,
Development of a High-Current Hydrogen-Negative Ion Source for LHD-NBI System; Aug.1998

NIFS-558 M. Tanaka, A. Yu Grosberg and T. Tanaka,
Molecular Dynamics of Structure Organization of Polyampholytes;Sep. 1998